Theory of a resonant level coupled to several conduction-electron channels in equilibrium and out of equilibrium

László Borda,[1] Károly Vladár,[2] and Alfréd Zawadowski[1,2]
[1]*Department of Theoretical Physics and Research Group "Theory of Condensed Matter" of the Hungarian Academy of Sciences, Budapest University of Technology and Economics, Budafoki út 8. H-1521 Budapest, Hungary*
[2]*Research Institute for Solid State Physics and Optics, P.O. Box 49, H-1525 Budapest, Hungary*
(Received 22 December 2006; published 12 March 2007)

The spinless resonant level model is studied when it is coupled by hopping to one of the arbitrary numbers of conduction-electron channels. The Coulomb interaction acts between the electron on the impurity and in the different channels. In the case of a repulsive or attractive interaction the conduction electrons are pushed away or attracted to ease or hinder the hopping by creating unoccupied or occupied states, respectively. In the screening of the hopping orthogonality catastrophe plays an important role. At equilibrium in the weak- and strong-coupling limits the renormalizations are treated by perturbative, numerical, and Anderson-Yuval Coulomb gas methods. In the case of two leads the current due to applied voltage is treated in the weak-coupling limit. The presented detailed study should help to test other methods suggested for nonequilibrium transport.

DOI: 10.1103/PhysRevB.75.125107 PACS number(s): 72.10.Fk, 73.63.Kv, 72.15.Qm

I. INTRODUCTION

In recent years the quantum impurity problem out of equilibrium has attracted great interest. The most relevant realizations are quantum dots connected to at least two metallic leads[1] and short metallic wires containing magnetic impurities.[2] In the impurity problem exact methods play distinguished roles especially the Bethe ansatz and conformal invariance. The generalization of these methods to out-of-equilibrium situations is the most challenging new directions. Mehta and Andrei are aiming to solve the Kondo problem on a dot with two contacts attached. First a simple resonant level without spin was studied to test the new generalization of the Bethe ansatz method.[3] Their elegant suggestion is very provocative. In order to test this kind of new methods we perform a detailed study of that problem using different weak-coupling perturbative methods combined with the renormalization group (NRG). As the final goal we calculate the current flowing through the impurity when a finite voltage is applied on the contacts. The most challenging claim of Mehta and Andrei is that the current is a nonmonotonic function of the strength of the Coulomb coupling between the electron on the dot and conduction electrons in the two leads.

In order to make the comparison more explicit we generalize the time-ordered scattering formalism for nonequilibrium in the next-leading logarithmic order. In this way the current is calculated as a function of the applied voltage and the Coulomb coupling strength. Increasing the Coulomb coupling strength we find also a nonmonotonic feature but the order of increasing and decreasing regions is the opposite to the finding of Mehta and Andrei.[3]

The model to be treated is the following: A single-impurity orbital is coupled to two reservoirs of Fermi gas via hopping but the two reservoirs have different chemical potentials μ_L and μ_R on the left and right of the impurity in a one-dimensional model. $\mu_L-\mu_R=eV$ is determined by the applied voltage V (e is the electronic charge). The Coulomb interaction acts between the electron on the impurity level and the conduction electrons at the impurity position. Thus the Hamiltonian has the form

$$H = H_0 + H_1 + H_2, \tag{1}$$

with

$$H_0 = \sum_{\substack{\alpha=L,R \\ k}} (k-k_\alpha) v_F a_{k\alpha}^\dagger a_{k\alpha} + \varepsilon_d d^\dagger d, \tag{2}$$

where $k>0$ and $k_L-k_R=eV/v_F$, v_F is the Fermi velocity, and $a_{k\alpha}^\dagger$ is the creation operator of the spinless Fermion in lead $\alpha=L/R$, while ε_d is the energy of the local level and $d^\dagger$ is the creation operator for the electron on that site. The interaction term is

$$H_1 = U\left(d^\dagger d - \frac{1}{2}\right)\left(\sum_{\alpha=L,R} a_\alpha^\dagger a_\alpha - \frac{1}{2}\right), \tag{3}$$

where U is the Coulomb coupling which in a physical case $U>0$, $a_\alpha=\frac{1}{\sqrt{L}}\Sigma_k a_{k\alpha}$, and L is the length of the chain. The existence of the substraction of $1/2$ is not essential; it can be omitted and then ε_d is shifted as $\varepsilon_d-U/2$ and a local potential $-\frac{1}{2}U$ is acting on the electrons, but the latter one can be taken into account by changing the electron density of states in the leads at the position of the impurity.

The hybridization between the lead electrons and the localized electron is described by

$$H_2 = V_\alpha \sum_\alpha (d^\dagger a_\alpha + a_\alpha^\dagger d), \tag{4}$$

where V_α is the hybridization matrix element.

In the case of equilibrium it is useful to generalize the model to N reservoirs instead of L, R, and then α runs through $\alpha=0,1,\ldots,N-1$ and $\mu_\alpha=\mu$. Then the hybridization term in H_2 is chosen in a specific form

$$H_2 = V_0(d^\dagger a_0 + a_0^\dagger d), \tag{5}$$

indicating that only the electrons with $\alpha=0$ are hybridizing while the others are taking part only in the Coulomb screen-

ing. Namely, only those electrons are hybridizing which have the symmetry of the localized orbital (s-like). As a result of the screening the electron gas is polarized depending on the occupation of the localized state and those polarizations lead to orthogonality catastrophe.[4]

The model with $N=1$ is known as a resonant level model and has been studied in great detail[5,6] and the one with $N \geq 1$ has been introduced to study finite- range interactions in three dimensions (3D).[7]

The goal of the present paper is to provide weak-coupling results for $V \neq 0$. But before doing that the $V=0$ equilibrium case is studied in the weak-coupling limit by the diagram technique. Then to extend the results are extended for stronger couplings of Wilson's numerical NRG[8] and Anderson-Yuval Coulomb gas method[9] is used in order to check the validity of weak-coupling results concerning a specific behavior. Namely, at some stage of the calculation in the exponent of the renormalized quantities a combination

$$-\varrho_0 U + \frac{1}{2} N (\varrho_0 U)^2 \tag{6}$$

appears. For $U>0$ this is changing sign at $\varrho_0 U = \frac{2}{N}$ and this leads in changing the increasing to decreasing behavior but this crossover is well beyond the validity of the perturbation theory at least for $N=2$.

In order to judge the real situation, an NRG study will be performed including the weak- $(\varrho_0 U \ll 1)$ as well as strong-coupling regions $\left(\varrho_0 U \geq \frac{2}{N}\right)$ to get insight into whether the crossover indicated above is expected or is likely an artifact of the weak-coupling theory. We also map the problem to a one-dimensional Coulomb model closely following the work of Anderson and Yuval, where the screening can even be in the strong-coupling limit. All of these methods suggest a coherent picture of the crossover, and they agree very well especially for $N=4$.

The study of such a crossover is especially relevant as in the work of Mehta and Andrei[3] such a crossover is suggested in the current flowing in the nonequilibrium case $V \neq 0$ at $\varrho_0 U \sim 2$. If we could find the crossover already in equilibrium, then it is obvious to expect the same in the nonequilibrium situation.

The paper is organized in the following way: In Sec. II we provide the analytical perturbative method up to next-to-leading logarithmic order, introducing extra channels for screening, where the nonmonotonic competion of the vertex and self-energy correction is already demonstrated in equilibrium. In Sec. III the equilibrium calculation is extended to strong coupling by using Wilson's numerical renormalization group technique and the result is compared to that of the analytical calculation. In Sec. IV the Anderson-Yuval method is presented. In Sec. V the time-dependent scattering method is applied for nonequilibrium closely following the generalized version of Anderson's poor man's scaling in the next to leading order and the current is calculated. In Sec. VI the results are summarized. In the Appendix some cancellation due to Ward indentities are discussed.

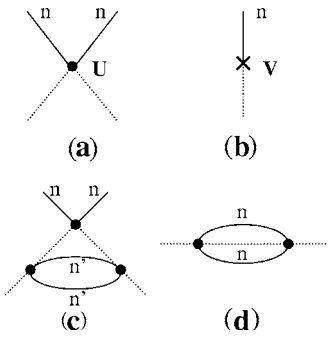

FIG. 1. Vertex diagrams (a), (b), (c) and the impurity self-energy (d). Solid lines stand for conduction-electron propagators while the dotted line for those of electron on the impurity level. The interactions are indicated by dots (U) and crosses (V). In the case of conduction electrons the channel indices are also indicated.

II. PERTURBATION THEORY: WEAK-COUPLING LIMIT

The resonant level model is given by Eqs. (1), (2), and (4). It does not contain noncommuting terms; thus, Kondo behavior is not expected in the weak-coupling limit. In the strong-coupling limit the model, however, can be mapped to an anisotropic Kondo model[5–7] but such mapping is not considered here. The model shows strong similarities to the x-ray absorption,[10,11] as the strength of the interaction (invariant charge) between conduction electrons and the electron on the impurity level is scale invariant. The system shows scaling in terms of the reduction of the conduction-electron bandwidth D. In the case $N=1$ the scaling equations were derived by Schlottmann[6] and those can be easily extended for arbitrary N.

There are two different kinds of vertex corrections depicted in Figs. 1(a)–1(c), where the solid lines stand for conduction electrons, the dotted line for electrons on the impurity level, and the interactions are indicated by dots (U) and crosses (V). In case of conduction electrons the channel indices are also indicated. The Hartree-Fock energy shift can be incorporated by ε_d. The self-energy of the electron on the impurity is depicted in Fig. 1(d). In the calculation of the self-energy counterterms are introduced to eliminate the constant terms to keep $\varepsilon_d=0$ unrenormalized. Closely following the earlier works,[6,12,13] the invariant charge for the Coulomb interaction takes the form

$$U_{\text{inv}} = \Gamma(\omega/D) d(\omega/D), \tag{7}$$

where Γ is the vertex function and

$$d(\omega/D) = G(\omega, D)(\omega - \varepsilon_d)$$

can be determined perturbatively starting with 1 where G is the renormalized one-electron Green's function. The functions $\Gamma(\omega)$ and $d(\omega)$ are

$$\Gamma(\omega) = 1 + N \varrho_0^2 U^2 \ln\left(\frac{D}{\omega}\right) + \cdots,$$

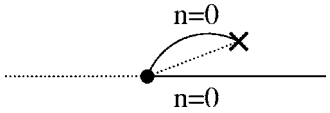

FIG. 2. Vertex correction to the hybridization.

$$d(\omega) = 1 - N\varrho_0^2 U^2 \ln\left(\frac{D}{\omega}\right) + \cdots, \tag{8}$$

where ϱ_0 is the conduction-electron density of states for spinless electrons in one of the channels $n=1,\ldots,N-1$. As the Coulomb interaction is independent of n, the factor N occurs. As the consequence of the Ward identity relating the vertex correction and the self-energy depicted in Figs. 1(c) and 1(d) cancel out in U_{inv},[6,10,11,13]

$$\frac{d}{d|\omega|}[\Gamma(\omega)d(\omega)] = \frac{d}{d|\omega|}U_{\text{inv}}(\omega) = 0; \tag{9}$$

thus, $U_{\text{inv}}=U$. The renormalization group gives

$$d(\omega) = \left(\frac{\omega}{D}\right)^{N\varrho_0^2 U^2} \tag{10}$$

for arbitrary n.

The hybridization contains the vertex correction for $n=0$ (Fig. 2),

$$V(\omega) = V\left(1 + U\varrho_0 \ln\frac{D}{\omega} + \cdots\right), \tag{11}$$

but it does not contain linear contribution in $\ln(D/\omega)$ in the order of U^2. The relevant invariant charge $V_{\text{inv}}(\omega)$ is

$$V_{\text{inv}}(\omega) = V(\omega)d^{1/2}(\omega) \tag{12}$$

as the interaction is connected by only one impurity line. Thus the terms linear in $\ln(D/\omega)$ are

$$V_{\text{inv}}(\omega) = V\left(1 + \varrho_0 U \ln\frac{D}{\omega} - \frac{1}{2}N(\varrho_0 U)^2 \ln\frac{D}{\omega} + \cdots\right). \tag{13}$$

The result of the renormalization equation is

$$V_{\text{inv}}(\omega) = V\left(\frac{\omega}{D}\right)^{-\varrho_0 U + N\varrho_0^2 U^2/2}. \tag{14}$$

The second term in the exponent appears as reduction of $V_{\text{inv}}(\omega)$ describing the Coulomb screening in the N channels.

For $U<0$ the $V_{\text{inv}}(\omega)$ interaction is always decreasing as ω is reduced but for $U>0$ it depends on the strength of U. For large enough U the screening dominates thus:

$$V_{\text{inv}}(\omega) = \begin{cases} \text{decreasing} & \text{for} \quad U\varrho_0 < 0, \\ \text{increasing} & \text{for} \quad 0 < U\varrho_0 < \dfrac{2}{N}, \\ \text{decreasing} & \text{for} \quad U\varrho_0 > \dfrac{2}{N}. \end{cases} \tag{15}$$

This behavior will be further discussed in Sec. VI.

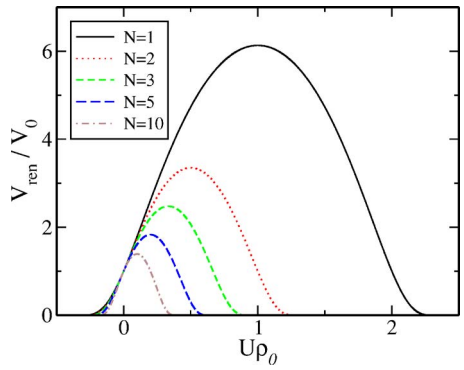

FIG. 3. (Color online) The renormalized hybridization as a function of $\varrho_0 U$ for different channel numbers. The intermediate maximum can diverge only for $\varrho_0 U=1$; in all the other cases, the increases are also rather moderate.

The scaling regions, however, are not unlimited as the impurity level has its own width Γ_{imp}. There are two contributions to the level width Γ_{imp}.

The hybridization broadens the impurity level just in case of the Anderson model and that is in second order in V:

$$\Gamma_{\text{imp}}(\omega) = \pi\varrho_0 V^2(\omega) = \pi\varrho_0 V\left(\frac{\omega}{D}\right)^{-2\varrho_0 U + N(\varrho_0 U)^2}, \tag{16}$$

where also the effect of renormalization is taken into account. There is also a Korringa-like broadening due to the creation of electron-hole pairs and thus $\Gamma_{\text{Korringa}} \sim U^2\omega$, where ω comes from the phase space. That is important only for large ω where everything is smooth and thus the broadening is not effective.

The broadening due to the hybridization cuts off the renormalization procedure at energy $\omega \sim \Gamma_{\text{imp}}(\omega)$. Combining Eqs. (14) and (16) and inserting the condition given above provides the final V_{ren} value as

$$\frac{V_{\text{ren}}}{V} = \left(\frac{V^2\varrho_0\pi}{D}\right)^{[-\varrho_0 U + N(\varrho_0 U)^2/2]/[1+2\varrho_0 U - N(\varrho_0 U)^2]}. \tag{17}$$

As shown in Fig. 3, for $U<0$ $V_{\text{ren}}/V<1$ renormalizes downwards and for even more negative U down to zero. For $U>0$ and $\varrho_0 U<2/N$ first V_{ren} increases with increasing U but for $\varrho_0 U>2/N$ it starts to decrease and tends to zero again. The intermediate maximum appears at $\varrho_0 U=1/N$. For $N=2$ that maximum is, however, already outside the weak-coupling limit, where the calculation cannot be trusted. The question still remains unanswered whether the nonmonotonic behavior for $U>0$ can be traced in strong-coupling calculations or not. The conclusions for the crossover might be trusted only for large $N \gg 1$, which does not have physical relevance.

III. NRG APPROACH FOR $V=0$

In order to determine the region of validity of the weak-coupling approach in equilibrium, we have performed a numerical (NRG)[8] analysis for the $N=2$ and $N=4$ cases.

In Wilson's NRG technique—after the logarithmic discretization of the conduction band—one maps the original

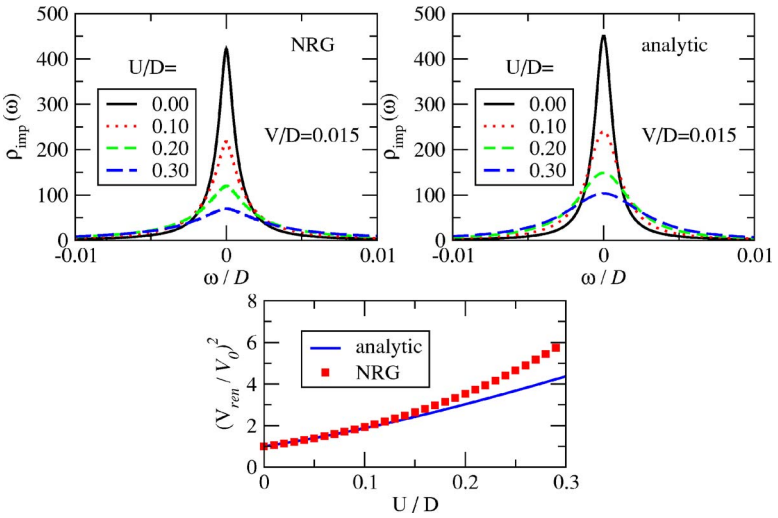

FIG. 4. (Color online) Upper panels: impurity density of states for $V/D=0.015$ and $U/D=0,\ldots,0.3$ as obtained by perturbative RG and Wilson's NRG. The lower panel shows the renormalized value of the hybridization, V_{ren}, as a function of the interaction strength U. The numerical data supports the weak-coupling results for $U/D \leq 0.2$.

Hamiltonian of an impurity problem to a semi-infinite chain with the impurity at the end of the chain. As a consequence of the logarithmic discretization the hopping amplitude along the chain decreases exponentially as $t_n \sim \Lambda^{-n/2}$ where $\Lambda > 1$ is a discretization parameter (we have used $\Lambda = 2$ throughout the calculations) while n is the site index. The separation of energy scales provided by the exponentially vanishing hopping amplitude allows us to diagonalize the Hamiltonian iteratively to approximate the ground state and the excitation spectrum of the full chain. Since we know the eigenenergies and eigenvectors of the Hamiltonian, we can calculate dynamical quantities such as the density of states using the Lehman representation of the spectral function.[8]

First let us focus on the physically relevant case of $U > 0$ and $N=2$. To compare the numerical data with the weak-coupling results, we have calculated the impurity density of states for different values of the interaction strength U. The results are shown in Fig. 4. The numerical data validate the weak-coupling results for $U/D \leq 0.3$. In our NRG calculation we considered a flatband with constant density of states $\varrho_0 = 1/2D$, where D stands for the half bandwidth. In the lower panel of Fig. 4 the renormalized value of the hybridization, V_{ren}, is shown as a function of the interaction strength U. In NRG calculations, we have defined V_{ren} from the finite-size spectrum directly. The finite-size spectrum as a function of iteration number crosses over from the initial fixed point to the strong-coupling one characterized by single-particle phase shifts $\delta = \pi/2$ at around M^*. M^* is determined by the renormalized hybridization, $\Delta_{\mathrm{ren}} = \pi V_{\mathrm{ren}}^2 \varrho_0 \sim \Lambda^{-M^*/2}$. We take $M = M^*$ when the energy of the first excited state exceeds 90% of its fixed-point value.

To answer the question whether an intermediate maximum appears outside the weak-coupling limit or not, we have performed calculations with very large values of the interaction strength up to $U/D = 5.0$. The results are shown in Fig. 5.

Our conclusion is that even for $N=2$ such a nonmonotonic behavior is found but the position of the maximum as well as the shape of the curve for large U differs essentially from those obtained by weak-coupling calculations. It still remains a question whether for case of many channels the weak-coupling calculation is reliable or not. To treat many channels with NRG is very challenging, but to see the tendency with increasing channel number, we performed the numerical analysis of the case $N=4$. The results are plotted in Fig. 5 as well. Our data suggest that already for $N=4$ the position of the turning point as well as the decay of the curve at large U is reproduced by the weak-coupling calculation with a much better accuracy than in case of $N=2$.

IV. ANDERSON-YUVAL APPROACH

In most of the physical cases the Coulomb interaction U dominates over the hopping term V_0. To overcome that difficulty, Yuval and Anderson[9] introduced a path integral method for the Kondo problem where the interaction U is described in terms of phase shifts while the hopping is treated as perturbation. The similarity between the Kondo and present problems can be exploited in the following way: The complex time axis is divided into intervals, and as is shown in Fig. 6 where the solid line represents the time interval when the impurity level is occupied and the light ones stand for unoccupied levels. The conduction electrons can join the time line at the end points of the intervals where hopping V_0 takes place while they can touch the time line at any other points due to the Coulomb interaction. Those are

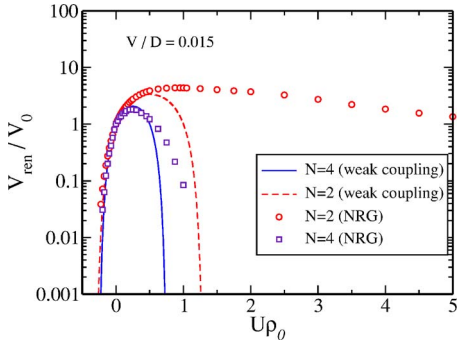

FIG. 5. (Color online) Comparison between weak-coupling RG and NRG approaches: the renormalized value of the hybridization, V_{ren} as a function of the interaction strength U for $N=2$ and $N=4$.

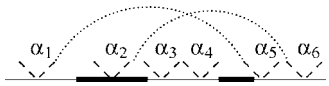

FIG. 6. The solid lines represents the time interval when the impurity level is occupied, and the light ones stand for unoccupied levels. The conduction electrons can join the time line at the end points of the intervals where hopping V_α takes place while they can touch the time line at any points due to the Coulomb interaction. Those are indicated by dashed lines which are labeled according to the channel indices α_i.

indicated by dashed lines which are labeled according to the channel indices α_i. Thus, the incoming and outgoing conduction-electron lines should be connected all possible ways, and finally a summation over all possible configuration of channel labelings α_i must be carried out. Some of the connections are indicated in Fig. 6 by dotted lines. The final result for the partition function can be given in analytical form as in Refs. 9 and 14 where the Kondo or the two-level system problems were treated. The partition function has the form of a one-dimensional Coulomb gas with appropriately defined vector charges C_α $(\alpha=1,\ldots,N-1)$. The scaling equations are derived by eliminating short time intervals at the short time cutoff τ with its initial value taken as the inverse bandwidth $\tau_0 \sim D^{-1}$. The interaction V_0 must be also made dimensionless by a factor $\sim \tau_0^{1/2}$.

The phase shifts for electrons in case of filled and empty impurity levels are $\delta_\alpha = -\arctan(\varrho_0 \pi U)$ and $\delta'_\alpha = -\arctan(\varrho_0 \pi U')$, respectively. Only their difference will appear in the scaling: $z_\alpha = (\delta_\alpha - \delta'_\alpha)/\pi$. The phase shifts are limited: $|\delta_\alpha|$, $|\delta'_\alpha| < \pi/2$. The Friedel sum rule requires $\Sigma_\alpha z_\alpha = -1$ which expresses that the one-electron difference between the filled and empty sites must be screened by charge oscillations formed by the conduction electrons. The hybridization can be associated with the fugacity:

$$y = V(\varrho_0 \tau_0)^{1/2} \cos\, \delta_0. \tag{18}$$

The interaction can be represented by charges at the interaction points as

$$C_\alpha^{\pm} = \pm (z_\alpha + \delta_{\alpha 0}), \tag{19}$$

where the index ± labels hopping in and out of the impurity level assisted by an electron annihilation or creation in channel 0.

The lengthy derivation of the scaling equations closely follows Refs. 14 and 15 and the final result is

$$\frac{dy}{d \ln \tau} = y\left(1 - \frac{1}{2}\sum_\alpha C_\alpha^2\right),$$

$$\frac{dC_\alpha}{d \ln \tau} = -2y^2 C_\alpha, \tag{20}$$

or expressed in terms of phase z (phase shifts) they are

$$\frac{dy}{d \ln \tau} = y\left(\frac{1}{2} - z_0 - \frac{1}{2}\sum_\alpha z_\alpha^2\right),$$

$$\frac{dz_\alpha}{d \ln \tau} = 2(\delta_\alpha 0 + z_\alpha) y^2. \tag{21}$$

Here the scaling is carried out by increasing τ to reduce the electronic bandwidth. The term $\frac{1}{2}y$ in the first line of Eq. (21) originates in the explicit factor $\tau_0^{1/2}$ in the definition of y, Eq. (18), and disappears from the corresponding scaling equation of V.

The system of equations (21) must be solved for initial values $y(\tau_0) \ll 1$ but z_α can be arbitrary. The fugacity can either increase or decrease exponentially depending on the quantity $\left(z_0 + \frac{1}{2}\Sigma_\alpha z_\alpha^2\right)$. Similar expressions were obtained in Ref. 7 by matching the perturbative results with expression in terms of phase shifts.

The regions for an attractive interaction and large enough repulsive one will be treated separately. In the first case $\left(-z_0 - \frac{1}{2}\Sigma_\alpha z_\alpha^2\right) < 0$ $(U<0, z_0>0)$. The solution is $y/y_0 = (\tau/\tau_0)^{-z_0 - \Sigma_\alpha z_\alpha^2/2}$, and thus y is decreasing; therefore, z_α $(\alpha = 0,\ldots)$ are slowly varying and thus the τ dependence can be ignored. Thus

$$V_{\text{inv}} = V_0 \left(\frac{\tau}{\tau_0}\right)^{-z_0 - \sum_\alpha z_\alpha^2/2}. \tag{22}$$

The situation is different for the repulsive interaction $(z_0<0)$. There are two regions in that case. In the first one $\left(-z_0 - \frac{1}{2}\Sigma_\alpha z_\alpha^2\right) > 0$ and y is increasing. Then Eq. (22) is valid as far as $y \ll 1$ is satisfied. There is, however, a crossover where $\left(-z_0 - \frac{1}{2}\Sigma_\alpha z_\alpha^2\right) = 0$ to the second region where y decreases again and the screening dominates. The larger N, the stronger the decrease is.

The crossover between the increasing and decreasing regions is at

$$z_0 = -\frac{1}{2}\sum z_\alpha^2.$$

As z_α's are very slightly renormalized, the unrenormalized values can be used and δ_α is independent of α $(\delta<0)$. Thus the crossover is at $z_\alpha = 2/N$ and then

$$N=2: \quad \delta = \frac{\pi}{2}: \quad \varrho_0 U \to \infty,$$

$$N=4: \quad \delta = \frac{\pi}{4}: \quad \varrho_0 U = \frac{1}{\pi}.$$

Comparing with the results of NRG in case $N=2$ the turning point is at $\varrho_0 U \to \infty$ and thus the agreement is not complete but at least it could be argued that it is inside the accuracy of the scaling equation. The weak-coupling scaling result is very poor as was expected (see Fig. 4). For $N=4$ all the methods give very similar results.

The general solution of the scaling equations can be searched in the form $C_\alpha(\tau) = (C_\alpha)_{\text{initial}} \zeta(\tau)$. Then

$$\frac{d\zeta}{d \ln \tau} = -2y^2 \zeta,$$

$$\frac{dy}{d\ln\tau} = \left(1 - \frac{1}{2}\zeta^2 \sum_\alpha C_\alpha^2\right) y. \tag{23}$$

The scaling trajectories are

$$4y^2(\tau) - \zeta^2(\tau)\sum_\alpha C_\alpha^2 + 4\ln\zeta(\tau) = 4y^2(0) - \sum_\alpha C_\alpha^2. \tag{24}$$

During the renormalization y is fast increasing and the scaling is stopped where it reaches unity. Meanwhile, ζ decreases slowly and its renormalized value can be extracted from Eq. (24). The result in leading order in y reads as

$$\ln\zeta(\tau) = -\frac{y^2(\tau) - y_0^2}{\frac{1}{2} - z_0 - \frac{1}{2}\sum_\alpha z_\alpha^2}. \tag{25}$$

Outside that region the long-time approximation for the conduction-electron Green's function cannot be applied.

V. WEAK-COUPLING APPROACH FOR OUT OF EQUILIBRIUM

Considering theoretical methods two ways can be followed: the Keldysh Green's function method or the calculation of the scattering amplitude by time-ordered perturbation theory. Here the second method will be followed, where the initial conduction-electron states can be arbitrary nonequilibrium states and for the intermediate and final states the actual nonequilibrium distributions are taken into account. This method has been earlier applied in the leading-logarithmic approximation,[16–18] which is a generalization of Anderson's poor man scaling.[19]

Here the extension of that method is presented to next leading order. For equilibrium first the Kondo model was treated that way.[20] The basic idea is to calculate the development of the initial $|i\rangle$ state to the final $|f\rangle$ one, but in second order the renormalization of the norms of those states must be corrected also. Thus the scattering matrix element to be considered is

$$T'_{fi}(\omega) = \frac{\langle f|H_{\rm int}\sum_{n=0}^{\infty}\left(\frac{1}{\omega - H_0}H_{\rm int}\right)^n|i\rangle}{\left[\langle f|\sum_{n=0}^{\infty}\left(\frac{1}{\omega - H_0}H_{\rm int}\right)^n|f\rangle\langle i|\sum_{n=0}^{\infty}\left(\frac{1}{\omega - H_0}H_{\rm int}\right)^n|i\rangle\right]^{1/2}}, \tag{26}$$

where ω is the initial energy of state $|i\rangle$ and the Hamiltonian is split as $H = H_0 + H_{\rm int}$. In the present problem the correction of the normalization occurs for the impurity electron states while in the Kondo model for the spin states. These normalizations appeared in the previous treatment as $d^{1/2}(\omega)$ in Eq. (12).

The scaling equation can be obtained after changing the cutoff $D \to D - \delta D$ by adjusting the coupling constant to keep T_{fi} invariant for appropriate $|i\rangle$ and $|f\rangle$. In the following we use the original left and right states ($\alpha = L, R$) with $V_L = V_R$ as a start. In order to derive the scaling for coupling U the initial and final states should be $a_k^\dagger d^\dagger|0\rangle$ where $|0\rangle$ is the nonequilibrium state at applied voltage eV, for which disregarding V the state is the noninteracting ground state. Considering the occupation n_d of the d level the occupation probability in the steady state must be determined in presence of eV. That value will be $\langle n_d\rangle = 1/2$ for $\varepsilon_d = 0$ but in the general case $\varepsilon_d \neq 0$ it can depend on eV. The diagrams of the numerator up to $\sim U^3$ order are shown in Figs. 7(i)–(vi) where the diagrams should be decorated by the direction of the lines in all possible ways. The diagram of the self-energy is shown in Fig. 7(vii). In logarithmic approximation only the diagrams linear in $\ln\frac{D}{\omega}$ are contributing to the scaling equations and thus the relevant vertex corrections are (ii), (v), and (vi) while (iii) and (iv) are not as these provide $\ln^2\frac{D}{\omega}$. The type (ii) diagrams with the parallel and antiparallel lines cancel each other. As the logarithmic terms in diagrams (v), (vi), and (vii) come from closed electron loops which are independent of the actual values of μ_L and μ_R, to the logarithmic term the left and right contacts contribute separately which should be independent of the applied voltage. That simplification is not sustained in higher-order contributions where the left and right lines simultaneously occur. The self-energy correction in (vi) contributes by adding it to either of the incoming and outgoing d lines. One of those corrections is canceled by the denominator in Eq. (26). As is well known from the spinless fermionic case—e.g., the x-ray absorption problem[11,13]—the remaining diagram is canceled by (v). Thus, the single-logarithmic term does not remain. This is similar to the equilibrium case [see Eq. (9)] and thus the invariant coupling $U_{\rm inv} = \text{const}$. (For the details see the Appendix).

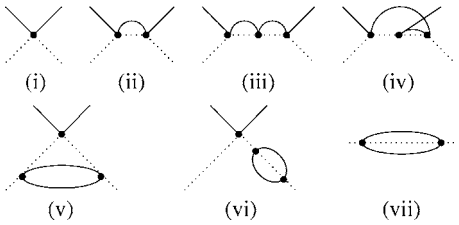

FIG. 7. Panels (i)–(vi): the diagrams up to $\sim U^3$ order contributing to the numerator of Eq. (26). The diagrams should be decorated by the direction of the lines in all possible ways. The diagram of the self-energy is shown in panel (vii).

In the following the renormalization of the hybridization depicted in Figs. 1(b) and 2 is crucial where, e.g., $|i\rangle = d^\dagger|0\rangle$ and $|f\rangle = a_{k\alpha}^\dagger|0\rangle$. Keeping terms up to $\sim VU^2$, after taking the denominator in Eq. (26) into account the final form of T_{fi} is

$$\langle 0|a_{k\alpha}Td^\dagger|0\rangle = V_\alpha\left(1 + U\varrho_0\ln\frac{D - \varepsilon_d}{\omega - \alpha\frac{eV}{2} - \varepsilon_d} - \frac{1}{2}U^2\varrho_0^2\ln\frac{D}{\omega - \varepsilon_d}\right), \tag{27}$$

where the first correction is due to the vertex depicted in Fig.

2, while the second one arises from the self-energy on the leg of diagram reduced by the denominator by a factor 1/2. This result agrees with Eq. (13) ($N=2$) at $eV=0$. Here taking the special case $\varepsilon_d=0$ the voltage eV serves as a low-energy cutoff.

As has been mentioned earlier considering the d level there is a steady-state occupation n_d. This value is determined from the balance of the inflow and outflow of the conduction electrons. To determine it for $\varepsilon_d \neq 0$ two other quantities must be known: namely, the changes in the level position and the spectral function of the d level, $\tilde{\varepsilon}_d$ and $\varrho_d(\varepsilon)$, due to the applied voltage. That calculation can be carried out numerically in a self-consistent way.

The probability of scattering of an electron coming from the left (L) or right (R) into the d level is denoted by $W^+_{L/R}$ while the opposite process by $W^-_{L/R}$. These quantities are

$$W^+_{L/R} = (1-n_d)2\pi\varrho_0 \int V^2_{L/R}(\varepsilon)\varrho_d(\varepsilon)f_{L/R}(\varepsilon)d\varepsilon \tag{28}$$

and

$$W^-_{L/R} = n_d 2\pi\varrho_0 \int V^2_{L/R}(\varepsilon)\varrho_d(\varepsilon)[1-f_{L/R}(\varepsilon)]d\varepsilon, \tag{29}$$

where $V_{L/R}(\varepsilon)$ are determined from renormalization group equations with the appropriate infrared cutoffs and $f_{L/R}(\varepsilon) = f(\varepsilon \pm eV/2)$ is the Fermi distribution function for the leads in the presence of the voltage. Those will be taken at zero temperature $T=0$.

The steady state is determined by

$$\frac{d}{dt}n_d = W^+_L + W^+_R - W^-_L - W^-_R = 0. \tag{30}$$

This equation combined with Eqs. (28) and (29) gives

$$n_d = \frac{\int \varrho_d(\varepsilon)[V^2_L(\varepsilon)f(\varepsilon+eV/2) + V^2_R(\varepsilon)f(\varepsilon-eV/2)]d\varepsilon}{\int \varrho_d(\varepsilon)[V^2_L(\varepsilon)+V^2_R(\varepsilon)]d\varepsilon}. \tag{31}$$

If electron-hole symmetry holds, $\varepsilon_d=0$, and then $n_d=1/2$. The next step is to determine the self-energy of the d electron. The d-electron propagator is

$$\langle 0|dH_1 \frac{1}{\omega - H_0} H_1 d^\dagger|0\rangle,$$

which can be simply developed because the occupied d level determines the time flow. The self-energy corrections appear also in the normalization. The effect of hybridization is just to give an extra broadening of the d level to be considered later. Without hybridization the self-energy is

$$\Sigma(\omega + i\delta) = U^2\varrho_0^2 \int_{-D+\mu}^{D+\mu} d\xi' \int_{-D+\mu}^{D+\mu} d\xi''[1-f(\xi'')]f(\xi') \times \frac{1}{\omega + \xi' - \xi'' - \varepsilon_d + i\delta}, \tag{32}$$

which can be evaluated as

$$\mathrm{Re}\,\Sigma(\omega) = U^2\varrho_0^2\left(|\omega-\varepsilon_d|\ln\frac{|\omega-\varepsilon_d|}{D} + 2D\ln 2\right), \tag{33}$$

and

$$\mathrm{Im}\,\Sigma(\omega) = \pi U^2\varrho_0^2(\omega-\varepsilon_d)\Theta(\omega-\varepsilon_d). \tag{34}$$

In the equilibrium calculation the term proportional to $\sim\omega$ is contributing to the function $d(\omega)$ in Eqs. (8) and the last constant term $\sim 2D\ln 2$ is eliminated by the applied counterterm to keep ε_d unrenormalized while $\mathrm{Im}\,\Sigma(\omega)$ is a Korringa type of relaxation. It is to be noted that the voltage does not occur as the energy goes directly into the electron-hole creation of the same electrode. As we mentioned at the end of Sec. II, this broadening is less important at small energies. The hybridization of the d level gives the essential part of the broadening just like in the Anderson impurity model

$$\Gamma(\varepsilon) = 2\pi\varrho_0[V^2_L(\varepsilon) + V^2_R(\varepsilon)], \tag{35}$$

where the voltage-dependent hybridization strength must be used.

The d-electron spectral function is

$$\varrho_d(\omega) = \frac{1}{\pi}\frac{\Gamma(\omega)/2}{(\omega-\varepsilon_d)^2 + [\Gamma(\omega)/2]^2}. \tag{36}$$

With the help of these quantities we are ready to calculate the current through the impurity:

$$I = \frac{1}{2}\frac{d}{dt}(N_R - N_L) = W^-_R + W^+_L - W^+_R - W^-_L. \tag{37}$$

Combining this equation with the expression of $W^\pm_{L/R}$ given in Eqs. (28) and (29) the current takes the form

$$I = n_d 2\pi\varrho_0 \int [V^2_R(\varepsilon) - V^2_L(\varepsilon)]\varrho_d(\varepsilon)d\varepsilon - 2\pi\varrho_0 \times \int [f(\varepsilon - eV/2)V^2_R(\varepsilon) - f(\varepsilon+eV/2)V^2_L(\varepsilon)]\varrho_d(\varepsilon)d\varepsilon. \tag{38}$$

The numerical calculation goes as follows: for a fixed value of eV we discretize the energy interval $\omega_i \in [-D+\mu, D+\mu]$ and calculate the renormalized hybridization $V_{L/R}(eV,\omega_i)$ and the impurity self-energy. The latter is evaluated in such a way that the renormalized d-level position zero $\tilde{\varepsilon}_d=0$. By performing a sum over ω_i we can calculate at the level occupation $n_d(eV)$ and the current $I(eV)$ for the given value of the voltage. The result is shown in Fig. 8 for $U/D = 0,\ldots,0.10$.

In that regime of U the weak-coupling RG gave good results in equilibrium (presented in Sec. III) and therefore one expects reliable results in out of equilibrium as well. As

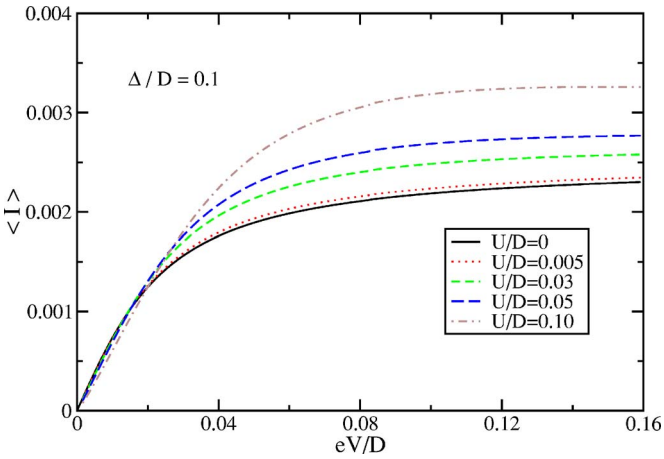

FIG. 8. (Color online) Current obtained by weak coupling RG for $\Delta/D=0.1$ and $U/D=0,0.005,0.03,0.05,0.10$. For this range of interaction strength the weak-coupling method was reliable in equilibrium.

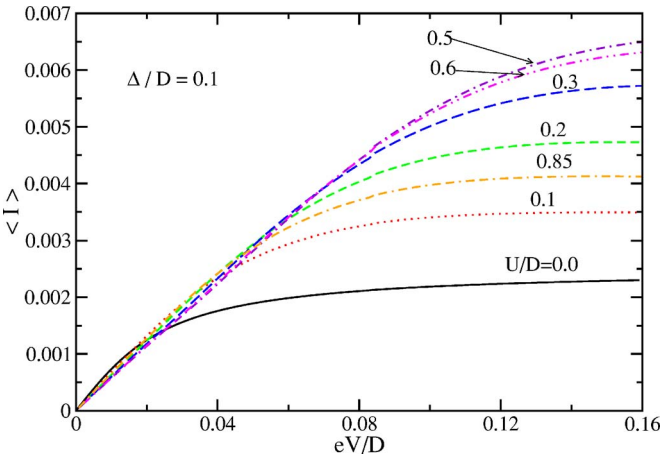

FIG. 9. (Color online) Current obtained by the scattering formalism for $\Delta/D=0.1$ and $U/D=0,0.10,0.20,0.30,0.50,0.60,0.85$. Note that the weak-coupling result is reliable for $U/D\leq 0.2$ only.

is shown in Fig. 8, the current increases with increasing interaction strength. The results can be interpreted as follows: with increasing U the impurity spectral function gets broadened since the hybridization is enhanced. In the linear regime ($eV<\Delta$) the U dependence drops out since the increase of coupling to the leads $\Gamma(eV,U)$ is canceled by the decrease of the height of the d level spectral function which scale as $\varrho_d(\omega=0)\sim 1/\Gamma(eV,U)$. For larger values of the voltage $eV>\Delta$ the d level is experienced not only at the peak of the spectral function $[\varrho_0(\omega=0)]$ and thus the current is not linear in eV any more. For $eV\gg\Delta$ the complete d level contributes to the current and thus it saturates and the asymptotic value is proportional to $\Gamma(eV,U)$.

VI. CONCLUSION

The resonant level model studied has very different behavior for attractive and repulsive interaction. This difference can be understood using the site representation for conduction electrons in the strong-U limit by the following argument.

(i) *In the case of attractive interaction* the particle on the d level attracts electrons to pile up around the impurity occupying the next site and thus the electron on the d level is blocked for hopping to the conduction band.

(ii) *In the case of repulsive interaction* the site next to the occupied d level is empty and thus that electron can easily jump to the conduction band.

All the methods predict that increasing the strength of an attractive interaction the hopping rate V is reduced and for strong enough coupling it even goes to zero (see Fig. 5 for $U\varrho_0<-0.25$). The effect of orthogonality catastrophe reducing the hopping is less relevant because that have been already reduced by the vertex correction.

In the repulsive case for large U the orthogonality catastrophe (self-energy correction) is reducing essentially the hopping rate. Thus the effective hopping V_{eff} is first enhanced by the effect described above and can reach a maximum which is followed by a reduction due to the orthogonality catastrophe. The position of the maximum can be pushed to lower energies by increasing the number of the screening channels, N, and thus the perturbative result becomes more and more reliable. In case of $N=2$ the latter method leads to a pronounced maximum but the NRG indicates only a slowly varying bump. In the Anderson-Yuval approach the maximum is even pushed to infinity. Thus the existence of the maximum is supported only by the NRG.

Considering the time-ordered scattering formalism the results are in accordance with the expectation of the weak-coupling result for $N=2$. The increasing U results in increasing current as first V is increased but for larger U due to the orthogonality catastrophe the current is essentially reduced (see Fig. 9). As the NRG does not give a sharp crossover for the hopping rate V_{eff}, the corresponding effect in the current must be less pronounced in reality. Of course, for $N\gg 2$ the crossover must clearly exist. Unfortunately, in the work of Mehta and Andrei the crossover is in the range of the reduced current, which is just the opposite of what is expected on the grounds of the physical picture established and results obtained by different methods for the hopping rate.

Very detailed further studies of the Bethe ansatz method are needed to understand and resolve the origin of the presented discrepancies.

ACKNOWLEDGMENTS

The authors acknowledge fruitful discussions with N. Andrei, P. Mehta, J. von Delft, J. Kroha, P. Wölfle, P. Schmitteckert, and G. Zaránd. This work was supported by Projects Nos. OTKA D048665, T048782, TS049881, and T046303. A.Z. is grateful to the Humboldt Foundation for support during his stay in Munich. L.B. acknowledges the support of a János Bolyai scholarship.

APPENDIX: CANCELLATION OF THE LOGARITHMIC TERMS IN THE RENORMALIZATION OF THE COULOMB INTERACTION

The diagrams of the numerator of Eq. (26) up to $\sim U^3$ order are shown in Figs. 7(i)–(vi) and the diagram of the

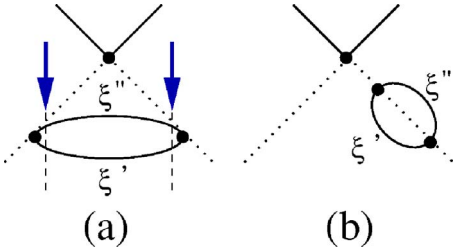

FIG. 10. (Color online) The two relevant diagrams up to $\sim U^3$ contributing to the numerator of Eq. (26). A Ward identity ensures the cancellation of these diagrams for small frequencies, meaning that no logarithmic term survives in second order and thus the invariant coupling U_{inv}=const.

self-energy is shown in Fig. 7(vii). As noted earlier, the logarithmic terms come from diagrams (v), (vi), and (vii). Note that the self-energy correction in (vi) [see also Fig. 10(b)] contributes by adding it to either of the incoming or outgoing d lines. One of those corrections is canceled by the diagram shown in Fig. 7(vii) in the denominator in Eq. (26). Therefore the two relevant diagrams are those depicted in Fig. 10. The contribution of Fig. 10(b) can be written as

$$\frac{1}{\omega-\varepsilon_d}U^2\varrho_0^2\int_{-D+\mu}^{D+\mu}d\xi'\int_{-D+\mu}^{D+\mu}d\xi''[1-f(\xi'')]f(\xi')\times\frac{1}{\omega+\xi'-\xi''-\varepsilon_d}. \tag{A1}$$

To get the purely logarithmic term we can now expand the integral in linear order in $\sim(\omega-\varepsilon_d)$ and get the form

$$U^2\varrho_0^2\int_{-D+\mu}^{D+\mu}d\xi'\int_{-D+\mu}^{D+\mu}d\xi''[1-f(\xi'')]f(\xi')\frac{1}{(\omega+\xi'-\xi''-\varepsilon_d)^2}. \tag{A2}$$

On the other hand, the contribution of Fig. 10(a) for small frequencies can be evaluated and the d-electron lines indicated by arrows occur twice just like the denominator squared in Eq. (A2). This Ward identity ensures the cancellation of the diagram shown in Fig. 7(v) by one of the leg ones in Fig. 7(vi). This means that no logarithmic term survives in second order and thus the invariant coupling U_{inv} =const.

[1] See, e.g., L. I. Glazman, and M. Pustilnik, in *Nanophysics: Coherence and Transport*, edited by H. Bouchiat *et al.* (Elsevier, Amsterdam, 2005), p. 427.
[2] See, e.g., N. O. Birge and F. Pierre, in *Fundamental Problems of Mesoscopic Physics, Interactions and Decoherence*, edited by I. V. Lerner, B. L. Altshuler, and Y. Gefen (Kluwer Academic, Dortrecht, 2004), p. 3.
[3] P. Mehta and N. Andrei, Phys. Rev. Lett. **96**, 216802 (2006).
[4] P. W. Anderson, Phys. Rev. Lett. **18**, 1049 (1967).
[5] See, e.g., P. B. Vigman and A. M. Finkel'stein, Zh. Eksp. Teor. Fiz. **75**, 204 (1978). [Sov. Phys. JETP **48**, 102 (1978)].
[6] P. Schlottmann, Phys. Rev. B **25**, 4815 (1982).
[7] T. Giamarchi, C. M. Varma, A. E. Ruckenstein, and P. Nozières, Phys. Rev. Lett. **70**, 3967 (1993).
[8] K. G. Wilson, Rev. Mod. Phys. **47**, 773 (1975); T. Costi, in *Density Matrix Renormalization*, edited by I. Peschel *et al.* (Springer, Berlin, 1999).
[9] G. Yuval and P. W. Anderson, Phys. Rev. B **1**, 1522 (1970).
[10] B. Roulet, F. Gavoret, and P. Nozières, Phys. Rev. **178**, 1072 (1969).
[11] P. Nozières and C. T. De Dominicis, Phys. Rev. **178**, 1097 (1969).
[12] M. Fowler and A. Zawadowski, Solid State Commun. **9**, 471 (1970); A. A. Abrikosov and A. A. Migdal, J. Low Temp. Phys. **3**, 319 (1970).
[13] J. Sólyom, J. Phys. F: Met. Phys. **4**, 2269 (1974).
[14] K. Vladár, A. Zawadowski, and G. T. Zimányi, Phys. Rev. B **37**, 2001 (1988). **37**, 2015 (1988).
[15] K. Vladár, Phys. Rev. B **44**, 1019 (1991).
[16] A. Zawadowski, in *Electronic Correlations: From Meso- to Nano-Physics*, edited by T. Martin, G. Montambaux, and J. Trân Thanh Vân (EDP Sciences, Paris, 2001), p. 389.
[17] A. Rosch, J. Paaske, J. Kroha, and P. Wölfle, Phys. Rev. Lett. **90**, 076804 (2003); J. Paaske, A. Rosch, and P. Wölfle, Phys. Rev. B **69**, 155330 (2004).
[18] O. Újsághy, A. Jakovác, and A. Zawadowski, Phys. Rev. B **72**, 205119 (2005).
[19] P. W. Anderson, J. Phys. C **3**, 2436 (1970).
[20] J. Sólyom and A. Zawadowski, J. Phys. F: Met. Phys. **4**, 80 (1974).